Raman scattering study of GaAs crystalline layers grown by molecular beam epitaxy at low temperature

H. Sano,[a] A. Suda, and T. Hatanaka
School of Materials Science, Japan Advanced Institute of Science and Technology, Tatsunokuchi, Ishikawa 923-1292, Japan

G. Mizutani
School of Materials Science, Japan Advanced Institute of Science and Technology, Tatsunokuchi, Ishikawa 923-1292, Japan and "Fields and Reactions," PRESTO, Japan Science and Technology Corporation, 4-1-8 Kawaguchishi-Honmachi, Saitama 332-0012, Japan

N. Otsuka
School of Materials Science, Japan Advanced Institute of Science and Technology, Tatsunokuchi, Ishikawa 923-1292, Japan

(Received 24 April 2000; accepted for publication 3 July 2000)

Raman scattering, x-ray diffraction, and transmission electron microscopy (TEM) were used to study GaAs layers grown by molecular beam epitaxy at low substrate temperatures (LT-GaAs). The intensity of forbidden Raman scattering of longitudinal optical and transverse optical phonons linearly increases as a function of the concentration of excess As in the range of $[As_{Ga}]=0.04\times10^{20}-1.175\times10^{20}\,cm^{-3}$. Concentrations of excess As in LT-GaAs layers were estimated from the lattice spacings measured with an x-ray diffractometer. No obvious defect was seen in cross-sectional TEM images of these nonstoichiometric As-rich GaAs layers. The origin of the forbidden Raman scattering of the nonstoichiometric LT-GaAs layers is explained as the strain induced by As_{Ga} (As antisite)-related defects with low structural symmetry. © *2000 American Institute of Physics.* [S0021-8979(00)10819-9]

I. INTRODUCTION

GaAs layers are grown by molecular beam epitaxy (MBE) normally at substrate temperatures around 600 °C.[1] When the substrate temperature during MBE growth is lowered to the range of 200–300 °C, the low temperature grown GaAs layers (LT-GaAs) contain excess As of around 1 at. % but still possess high crystalline quality.[2,3] As-grown and annealed LT-GaAs has novel electrical and optical properties. Namely, it has high electrical resistivity,[4,5] and its photogenerated carriers have an ultrashort lifetime of a few 100 fs.[6,7]

The novel physical properties of as-grown LT-GaAs result from point defects related to excess As.[8] Earlier studies indicate the existence of a number of types of excess As defects. It is, however, now believed that the dominant type of defects is antisite As(As_{Ga}), while a lower concentration of Ga vacancies (V_{Ga}) is also present.[9] The existence of only these two types of excess As defects has so far been experimentally confirmed without ambiguity; antisite As atoms are identified by near-infrared absorption (NIRA),[10,11] and Ga vacancies are detected by slow positron annihilation.[12] The existence of a high concentration of interstitial As atoms (As_i) was suggested by an earlier study which utilized ion channeling measurements,[13] but later it was shown by the same group that the results of the ion channeling measurements were also explained by the existence of only antisite As atoms. From the linear correlation between the antisite As concentration and lattice expansion it was concluded that antisite As is the dominant defect in LT-GaAs.[11] There is still the possibility of the existence of low concentrations of excess As defect complexes, one of which is suggested by the first principle calculations.[14]

The major potential area for the application of LT-GaAs and its related material, LT-InGaAs, is ultrafast all optical switching devices.[15,16] This is because the development of ultrafast all optical switches with switching speeds shorter than 1 ps is essential for the realization of future Tbit/s optical communication systems and LT-GaAs and LT-InGaAs are considered as important candidate materials for this goal. At the present stage, however, further studies of LT-GaAs and LT-InGaAs, in particular studies of excess As defects which serve as carrier trapping sites, are necessary in order to explore the above-mentioned possibility of the application.

Several methods have been used to study defects in such crystals. Since Raman scattering, as well as x-ray diffraction (XRD) and transmission electron microscopy (TEM), is a powerful technique for analyzing the structure of defects in a crystal, several Raman measurements of LT-GaAs have already been reported.[17,18] Unfortunately, these studies are not sufficiently systematic that we can find an intrinsic tendency in them. In some of them, even the concentrations of excess As in the samples were not estimated, and the crystal quality of the samples was not well characterized.

In the present study, we have characterized the defects and the strain in the LT-GaAs layers by Raman scattering, XRD, and TEM. We have grown a number of LT-GaAs

[a]Author to whom correspondence should be addressed; electronic mail: h-sano@jaist.ac.jp

layers, systematically controlling the concentration of excess As. Then, we have checked the crystallinity of the samples by TEM, and estimated the concentration of excess As by measuring the increase of lattice spacings with an x-ray diffractometer. We have found that the intensity of forbidden Raman scattering of longitudinal optical (LO) and transver optical (TO) phonons linearly increases as a function of the concentration of excess As. We suggest that this forbidden Raman scattering is due to As_{Ga}-related defects with low structural symmetry, which has a significant implication as to the nature of these excess As defects.

II. EXPERIMENT

Details of the method of growth of LT-GaAs layers are described elsewhere.[19] A semi-insulating GaAs(100) wafer was used as a substrate. In order to make LT-GaAs samples with various concentrations of excess As, we carefully controlled both the substrate temperature and the As_4/Ga flux ratio. The temperature of the substrate surface was measured by an infrared pyrometer within an error of 1 °C. Four different temperatures, 210, 240, 270, and 290 °C, were employed. The As_4/Ga flux ratio was set by controlling the temperature of effusion cells containing As and Ga. The As_4 and Ga fluxes in beam equivalent pressure (BEP) were measured with an ionization gauge placed at the position of the sample substrate.[19] The temperature of the effusion cells was stabilized for more than 2 h prior to each growth. All LT-GaAs layers were grown to a thickness of 640 nm at a growth rate of 0.9 μm/h.

In order to estimate the concentration of excess As in LT-GaAs layers, we have measured lattice spacings in the growth direction by XRD. Since an As–As bond is slightly longer than an As–Ga bond, excess As leads to lattice expansion in LT-GaAs.[11] According to an earlier report,[11] the change of lattice spacings ($\Delta d/d$) varies linearly as a function of the concentration of the As antisite. In the present study, we used the equation empirically determined by Liu *et al.*[11] to estimate the concentration of the As antisite [As_{Ga}]. The change of lattice spacings ($\Delta d/d$) was determined by rocking curve measurements of the 400 reflection using an x-ray diffractometer with a four crystal monochromator. Cu $K\alpha$ radiation was used for the measurements. Figure 1 shows one of the observed rocking curves as an example. The peaks at 0 and −161 arcsec are the 400 reflections of the substrate GaAs and LT-GaAs layers, respectively. In this example, $\Delta d/d = 1.18\times10^{-3}$ was obtained from the positions of the two diffraction peaks. From this value, we have obtained $[As_{Ga}] = 9.52\times10^{19}\,cm^{-3}$. The concentration of excess As of other samples were estimated in the same way.

Raman spectra of LT-GaAs layers were measured in quasibackscattering geometry. The incident light was the 488 nm line of an argon ion laser. In order to avoid the heating effect by laser light illumination, the power density of the laser beam on the sample surface was set at a value of 0.64 W/mm^2. The incident angle was 30° from the surface normal. Scattered light was collected with a set of lenses in the direction normal to the sample surface, passed through a notch filter and a single monochromator, and finally detected by a charge-coupled device (CCD) camera with an image intensifier. The resolution of the monochromator was set at about 10 cm^{-1}. All Raman experiments were performed in air at room temperature.

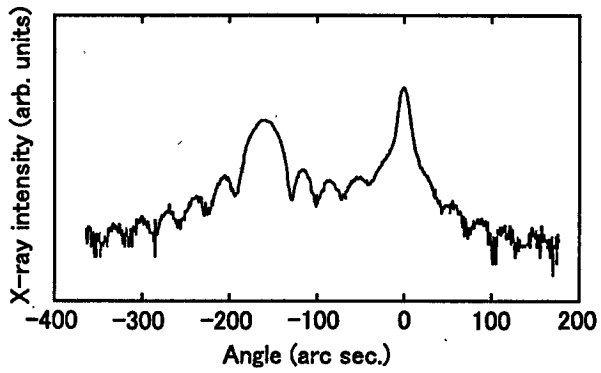

FIG. 1. Rocking curve of the 400 reflection of a LT-GaAs layer on a GaAs substrate. The peaks at 0 and −161 arcsec are the 400 reflections of the substrate and the LT-GaAs layer, respectively. From the positions of these diffraction peaks, the concentration of excess As of this sample is estimated to be $9.52\times10^{19}\,cm^{-3}$.

Polarized Raman spectra with four polarization combinations, shown in Table I, were obtained. Table I also shows the selection rule of LO- and TO-phonon Raman bands. This selection rule is derived from the Raman tensors,

$$\begin{pmatrix} 0 & 0 & 0 \\ 0 & 0 & a \\ 0 & a & 0 \end{pmatrix}, \begin{pmatrix} 0 & 0 & a \\ 0 & 0 & 0 \\ a & 0 & 0 \end{pmatrix}, \begin{pmatrix} 0 & a & 0 \\ a & 0 & 0 \\ 0 & 0 & 0 \end{pmatrix}, \quad (1)$$

for phonons polarized along the x, y, and z cubic axes, respectively.[20]

For TEM observation, several cross-sectional samples of LT-GaAs layers were prepared. These cross sections were observed with the bright field imaging mode at an acceleration voltage of 300 kV.

III. RESULTS AND DISCUSSION

Raman spectra of LT-GaAs layers with different concentrations of excess As, 0.00×10^{20}, 0.04×10^{20}, and $1.175\times10^{20}\,cm^{-3}$, are shown in Figs. 2(a)–2(c), respectively. The first sample, i.e., the LT-GaAs layer without excess As, is called the "stoichiometric LT-GaAs layer" in this article. Here, stoichiometric layer means that its lattice spacings are the same as those of the GaAs substrate within the detection

TABLE I. Polarization configurations and selection rule in backscattering from the (100) face of a GaAs crystal.

	Polarization		Selection rule of first-order Raman scattering	
Configuration	Incidence	Output	LO	TO
A	[011]	[01$\bar{1}$]	Forbidden	Forbidden
B	[011]	[011]	Allowed	Forbidden
C	[010]	[010]	Forbidden	Forbidden
D	[010]	[001]	Allowed	Forbidden

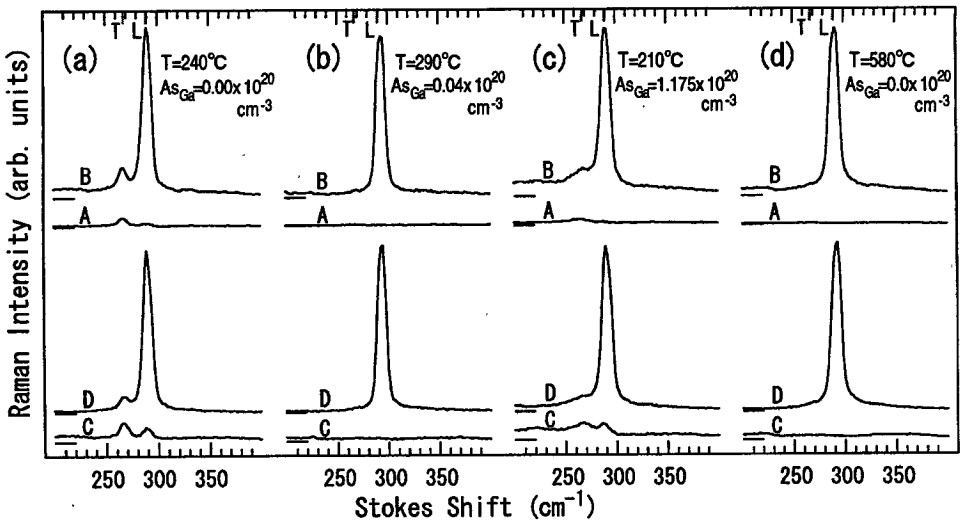

FIG. 2. Raman spectra of LT-GaAs layers with three different concentrations of excess As: $[As_{Ga}]$ =(a)0.00×10^{20}, (b) 0.04×10^{20}, and (c) $1.175\times10^{20}\,cm^{-3}$, and (d) a GaAs layer grown under normal MBE growth conditions. The four Raman spectra, A, B, C, and D, shown in (a)–(d) correspond to the spectra in the four polarization configurations shown in Table I, respectively.

limit of the x-ray diffraction technique. In Fig. 2(d), Raman spectra of the GaAs layer grown at a normal substrate temperature of 580 °C are shown as a reference. This last sample is called "the normal sample" in this article.

The Raman spectra of the normal sample perfectly obey the selection rule of the first-order Raman scattering from a T_d-symmetry crystal shown in Table I. Namely, the LO-phonon band at 290 cm^{-1} is seen only in polarization configurations B and D, and no TO-phonon band is seen in any of the four configurations. The Raman spectra of the LT-GaAs layer with $[As_{Ga}]=0.04\times10^{20}\,cm^{-3}$ in Fig. 2(b) are quite similar to those of the normal sample.

On the other hand, an obvious violation of the Raman selection rule is seen in the Raman spectra of LT-GaAs layers with $[As_{Ga}]=0.00\times10^{20}\,cm^{-3}$ [Fig. 2(a)] and $1.175\times10^{20}\,cm^{-3}$ [Fig. 2(c)]. In Figs. 2(a) and 2(c), a forbidden LO-phonon band is seen in polarization configuration C and a forbidden TO-phonon band is seen at ~268 cm^{-1} in all four configurations. The bandwidth of the observed forbidden TO-phonon bands in Fig. 2(a) is close to the instrumental resolution of ~10 cm^{-1}, while the bandwidth of the TO-phonon band in Fig. 2(c) is broader, i.e., 15–20 cm^{-1}.

Figures 3(a) and 3(b) show the intensities of the forbidden LO- and TO-phonon Raman scattering, respectively, as a function of the concentration of As_{Ga}. The vertical axes are Raman intensities of LO- and TO-phonon bands in configuration C normalized to the intensity of the LO-phonon band in configuration D for each sample. Different symbols in Fig. 3 represent different substrate temperatures adopted during MBE growth.

In Fig. 3, the intensity of forbidden Raman scattering increases in proportion to the concentration of As_{Ga}. As an exception, LT-GaAs layers with $[As_{Ga}]=0.00\times10^{20}\,cm^{-3}$, i.e., the stoichiometric LT-GaAs layer, show large forbidden Raman scattering. We also find that the intensities of forbidden Raman scattering of LT-GaAs with excess As depend not on the substrate temperatures during MBE growth, but only on the concentration of As_{Ga}.

Before turning to a detailed discussion of the origin of the observed violation of the Raman selection rule, we explain the results of TEM and XRD measurements employed to check the crystal quality. Figures 4(a) and 4(b) are different parts of the cross-sectional TEM images of a stoichiometric LT-GaAs sample with $[As_{Ga}]=0.00\times10^{20}\,cm^{-3}$. A high density of dislocations and stacking faults is seen in Fig. 4(a). In Fig. 4(b), we find a Ga droplet with the diameter of a few 10 nm at the surface. This TEM image in Fig. 4(b) indicates that slightly excess Ga atoms were present on the surface during MBE growth and these excess Ga atoms have

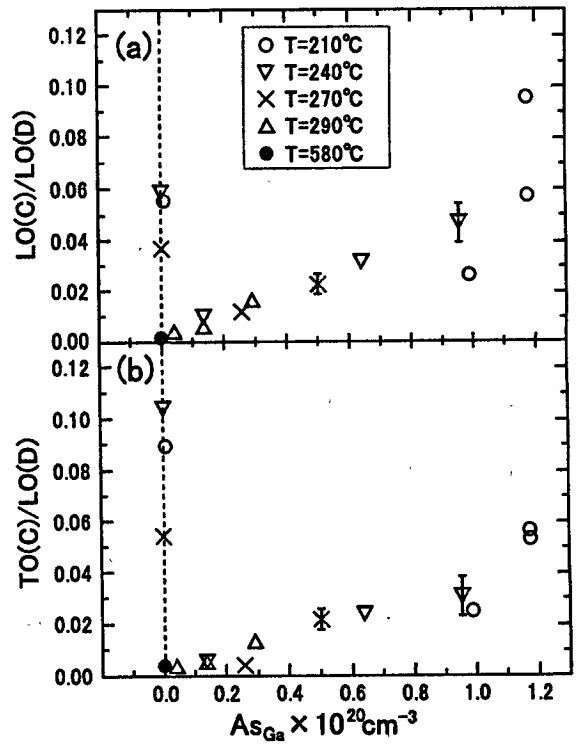

FIG. 3. Intensity of forbidden Raman scattering as a function of the concentration of excess As. (a), (b) Forbidden LO- and TO-phonon Raman intensities, respectively, in polarization configuration C. Both forbidden Raman intensities are normalized to the intensity of the LO-phonon band in configuration D for every sample. The symbols represent substrate temperatures during MBE growth, shown in the inset. The vertical dashed lines indicate the zero position of the concentration of excess As. The data on the dashed lines were obtained from samples, which were considered to be stoichiometric according to x-ray diffraction.

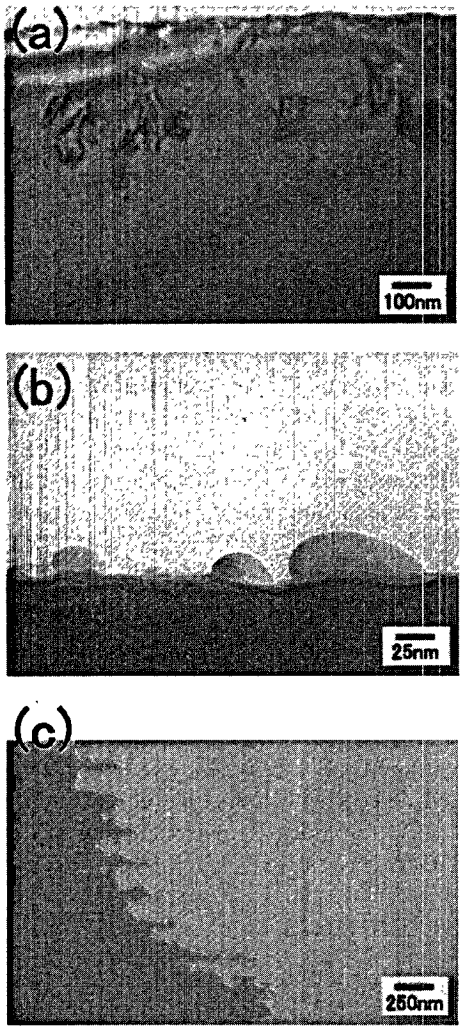

FIG. 4. Cross-sectional TEM images of LT-GaAs layers with $[As_{Ga}]$=(a), (b) 0.00×10^{20} and (c) $0.04\times10^{20}\,cm^{-3}$.

formed Ga droplets without being incorporated into the GaAs layer. Some excess Ga atoms, however, are incorporated into the layer, form liquid clusters, and then become the seeds inducing the creation of the dislocations and the stacking faults during MBE growth. In the XRD patterns of the same sample, we failed to see the effect of these extended defects, because the peak of the (400) reflections of the stoichiometric LT-GaAs layer precisely overlapped the peak of the substrate.

Figure 4(c) is a cross-sectional TEM image of the LT-GaAs layer with $[As_{Ga}]=0.04\times10^{20}\,cm^{-3}$. No extended defects such as dislocations and stacking faults are seen in Fig. 4(c). The LT-GaAs layers containing much more excess As show similar TEM images.

In the XRD patterns of these LT-GaAs layers with excess As like the one in Fig. 1, the peak width of the (400) reflection corresponds to the reciprocal of the thickness of the LT-GaAs layer. Furthermore, clear fringes are seen in the XRD profiles. The fringes are due to the interference of x rays reflected at the upper and lower interfaces of the LT-GaAs layer. These observations imply that the lattice structure of the LT-GaAs crystal is well ordered and that the LT-GaAs layer has flat and abrupt interfaces. From the above TEM and XRD measurements, we conclude that the crystallinity of the nonstoichiometric LT-GaAs layers which were grown for this study is excellent even if the concentration of excess As exceeds $1.0\times10^{20}\,cm^{-3}$.

Let us now consider the origin of the observed violation of the Raman selection rule. In the case of the stoichiometric LT-GaAs layers, it is clear that the dislocations and the stacking faults observed in Fig. 4(a) are the origin of the violation of the Raman selection rule. Hence, we do not discuss this stoichiometric sample any further in the present article.

On the other hand, there must be some origin of the violation of the Raman selection rule of the LT-GaAs layers with high concentration of excess As other than the poor crystallinity, because they are high quality epitaxial films. Possible candidates of the origin are (1) surface roughness, (2) band bending, (3) uniaxial strain, and (4) point defects with low structural symmetry. In the following, we will discuss the feasibility of each candidate.

First, we examine whether the roughness of the GaAs surface induces a violation of the Raman selection rule by depolarizing the incident and scattered light. This effect is excluded for the following reason. If this depolarization effect of surface roughness is operative, the intensity of forbidden Raman scattering in polarization configuration *A* is expected to be almost the same as that in configuration *C*. However, Fig. 2(c) shows that the Raman intensity in configuration *A* is much smaller than that in configuration *C*. Thus, the effect of surface roughness is not operative in the present study. This explanation is also supported by the independence of the intensities of the forbidden Raman scattering on the growth temperature, since a lower growth temperature normally results in a rougher surface due to reduced surface atom migrations.

Second, we consider the effect of band bending. It is well known that a strong electric field near the surface arising from band bending induces modification of the Raman selection rule. In the case of GaAs(110) surfaces, the forbidden LO-phonon Raman band can be seen by electric-field-induced Raman scattering (EFIRS).[21,22] However, an analysis of the Raman selection rule indicates that the electric field along the surface normal does not induce forbidden TO-phonon Raman scattering in the case of a GaAs(100) surface.[22] Thus, we conclude that EFIRS arising from band bending is not the origin of the violation of the Raman selection rule.

Third, we consider the change of symmetry of the crystal structure due to strain. LT-GaAs layers are uniaxially strained films. Namely, the unit cell of the LT-GaAs layers is expanded in the [100] direction as described in Sec. II. This strain leads to a change in symmetry of the GaAs crystal structure from T_d to D_{2d}, and the Raman tensor should change accordingly. The Raman tensor of a crystal with D_{2d} symmetry is given by

$$\begin{pmatrix}0&0&0\\0&0&b\\0&b&0\end{pmatrix},\begin{pmatrix}0&0&a\\0&0&0\\a&0&0\end{pmatrix},\begin{pmatrix}0&a&0\\a&0&0\\0&0&0\end{pmatrix}\quad(a\neq b),\qquad(2)$$

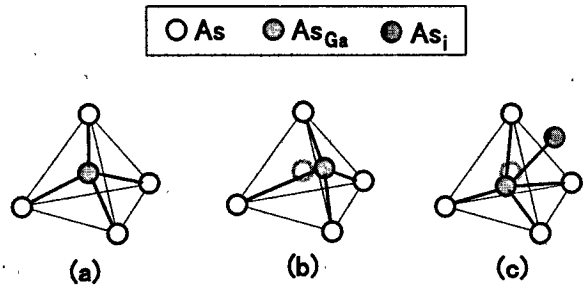

FIG. 5. Antisite As related defects: (a) the isolated As_{Ga} with T_d symmetry, (b) the isolated As_{Ga} with the symmetry reduced from T_d, and (c) the As_{Ga}-related complex with low structural symmetry. The gray open circles in (b) and (c) correspond to the normal antisite.

for phonons polarized along the x, y, and z cubic axes, respectively.[20] Equations (1) and (2) indicate that Raman intensities of optical phonon modes in both crystals with symmetry T_d and D_{2d} obey the same Raman selection rule. Hence, violation of the Raman selection rule due to uniaxial strain is not expected.

Fourth, let us consider the local strain induced around the excess As atoms in the LT-GaAs layer. It is reported that a large number of As antisites (As_{Ga}) exist in the LT-GaAs layer.[11] When the As_{Ga} is isolated and located at the equivalent position of the Ga atom in a perfect GaAs crystal, local strain around the As_{Ga} should exhibit the T_d symmetry [Fig. 5(a)]. Here, local strain around the As_{Ga} implies that nearest neighbor As atoms are centrosymmetrically displaced with respect to the antisite As atom. Thus, this local strain does not affect the ratio of the Raman tensor elements.

The above discussion leaves us only one remaining candidate to examine, namely, point defects with low structural symmetry. When the local strain exhibits low symmetry, some zero components in the Raman tensor shown in Eq. (1) become nonzero, and consequently the Raman selection rule will change. Thus, forbidden TO- and LO-phonon bands of GaAs(100) will be observed. The existence of the As_{Ga}-related complexes with low structural symmetry was proposed by Landman *et al.* through first-principle molecular dynamics calculations.[14] Yu *et al.* also proposed a similar complex defect with the C_{3v} symmetry from sharp-line photoluminescence spectra.[23] Therefore, we suggest that the As_{Ga}-related defect with low structural symmetry is the major origin of the observed violation of the Raman selection rule.

The most probable defect with low structural symmetry, however, is the isolated antisite As atoms. As suggested earlier by Liu *et al.*,[11] a larger bond length between the antisite As atom and nearest neighbor As atom may cause displacement of the four nearest neighbor As atoms which results in lowering the symmetry of the five As atom complex from the T_d symmetry. A picture of such an antisite As defect is shown in Fig. 5(b). If this is the case, one can easily explain the proportionality of the intensities of forbidden Raman scattering to the concentration of antisite As.

Another possibility is the coexistence of isolated As_{Ga} with T_d symmetry and As_{Ga}-related complexes with low structural symmetry such as shown in Fig. 5(c). Because the forbidden Raman intensity of the LT-GaAs layers with excess As increases in proportion to the concentration of the total As_{Ga} defects, we may assume that the concentration of the As_{Ga}-related complexes with low structural symmetry [LS-As_{Ga}] is proportional to the concentration of the total As_{Ga} defects [As_{Ga}]. Namely, the ratio of [LS-As_{Ga}] to [As_{Ga}] is constant in all the samples with excess As. In order to clarify which of the above two explanations is correct, further studies are necessary.

IV. CONCLUSION

We have grown LT-GaAs layers with various concentrations of excess As by MBE and have measured Raman scattering of LO- and TO-phonon modes of the LT-GaAs samples. The intensity of forbidden Raman scattering linearly increases as a function of the concentration of excess As in the range of $[As_{Ga}]=0.04\times10^{20}-1.175\times10^{20}\,cm^{-3}$. As an exception, the stoichiometric LT-GaAs layer without excess As shows large forbidden Raman scattering. The origin of the forbidden Raman scattering of the stoichiometric LT-GaAs layer is the dislocations and the stacking faults in the LT-GaAs layer. In the case of nonstoichiometric LT-GaAs layers with excess As, crystallinity is excellent even if the concentration of excess As exceeds $1.0\times10^{20}\,cm^{-3}$. As_{Ga}-related defects with low structural symmetry are suggested to cause forbidden Raman scattering in nonstoichiometric LT-GaAs layers.

ACKNOWLEDGMENTS

The authors would like to acknowledge valuable discussions with Professor S. Ushioda of Tohoku University. This work was supported in part by a Grant-in-Aid for Scientific Research from the Ministry of Education, Science, Sports and Culture.

[1] E. C. Larkins and J. S. Harris, Jr., in *Molecular Beam Epitaxy*, edited by R. F. C. Farrow (Noyes, Park Ridge, NJ, 1995), p. 114.
[2] M. Kaminska, E. R. Weber, Z. Liliental-Weber, R. Leon, and Z. U. Rek, J. Vac. Sci. Technol. B **7**, 710 (1989).
[3] M. R. Melloch, N. Otsuka, J. M. Woodall, A. C. Warren, and J. L. Freeouf, Appl. Phys. Lett. **57**, 1531 (1990).
[4] T. Murotani, T. Shimanoe, and S. Mitsui, J. Cryst. Growth **45**, 302 (1978).
[5] N. X. Nguyen and U. K. Mishra, in *Properties of Gallium Arsenide*, 3rd ed., edited by M. R. Brozel and G. E. Stillman (INSPEC, London, 1996), p. 689.
[6] S. Gupta, M. Y. Frankel, J. A. Valdmanis, J. F. Whitaker, and G. A. Mourou, F. W. Smith, and A. R. Calawa, Appl. Phys. Lett. **59**, 3276 (1991).
[7] J. F. Whitaker, in Ref. 5, p. 693.
[8] D. C. Look, in Ref. 5, p. 684.
[9] M. Luysberg, H. Sohn, A. Prasad, P. Specht, Z. Liliental-Weber, E. R. Weber, J. Gebauer, and R. Krause-Rehberg, J. Appl. Phys. **83**, 561 (1998).
[10] Z. Liliental-Weber, W. Swider, K. M. Yu, J. Kortright, F. W. Smith, and A. R. Calawa, Appl. Phys. Lett. **58**, 2153 (1991).
[11] X. Liu, A. Prasad, J. Nishio, E. R. Weber, Z. Liliental-Weber, and W. Walukiewicz, Appl. Phys. Lett. **67**, 279 (1995).
[12] D. E. Bliss, W. Walukiewicz, J. W. Ager, E. E. Haller, K. T. Chan, and S. Tanigawa, J. Appl. Phys. **71**, 1699 (1992).
[13] K. M. Yu, M. Kaminska, and Z. Liliental-Weber, J. Appl. Phys. **72**, 2850 (1992).
[14] J. I. Landman, C. G. Morgan, and J. T. Schick, Phys. Rev. Lett. **74**, 4007 (1995).
[15] I. Lahiri, D. D. Nolte, E. S. Harmon, M. R. Melloch, and J. M. Woodall, Appl. Phys. Lett. **66**, 2519 (1995).

[16] R. Takahashi, Y. Kawamura, and H. Iwamura, Appl. Phys. Lett. **68**, 153 (1996).
[17] Several Raman studies on LT-GaAs are summarized in H. Abe, H. Harima, S. Nakashima, and M. Tani, Jpn. J. Appl. Phys., Part 1 **35**, 5955 (1996).
[18] R. S. Berg, N. Mavalvala, T. Steinberg, and F. W. Smith, J. Electron. Mater. **19**, 1323 (1990).
[19] A. Suda and N. Otsuka, Appl. Phys. Lett. **73**, 1529 (1998).
[20] The Raman tensor of T_d and D_{2d} crystals was reported in R. Loudon, Adv. Phys. **16**, 345 (1978).
[21] Y. Kondo, G. Mizutani, K. Sakamoto, and S. Ushioda, Mater. Sci. Eng., B **7**, 177 (1990).
[22] G. W. Rubloff, E. Anastassakis, and F. H. Pollak, Solid State Commun. **13**, 1755 (1973).
[23] P. W. Yu, D. C. Reynolds, and C. E. Stutz, Appl. Phys. Lett. **61**, 1432 (1992).